NONLINEAR MAGNETIC PHENOMENA IN HIGHLY POLARIZED TARGET MATERIALS

Yu.F. Kiselev[1†] and W. Meyer[2]

(1) *CERN CH-1211, Geneve 23, Suisse/Switzerland*
† *E-mail: Yury.kiselev@cern.ch*
(2) *Physics Department, University of Bochum, 44780 Bochum, Germany.*

(On behalf of COMPASS Collaboration)

Abstract

The report introduces and surveys nonlinear magnetic phenomena which have been observed at high nuclear polarizations in polarized targets of the SMC and of the COMPASS collaborations at CERN. Some of these phenomena, namely the frequency modulation effect and the distortion of the NMR line shape, promote the development of the polarized target technique. Others, as the spin-spin cross-relaxation between spin subsystems can be used for the development of quantum statistical physics. New findings bear on an electromagnetic noise and the spectrally resolved radiation from LiD with negatively polarized nuclei detected by low temperature bolometers. These nonlinear phenomena need to be taken into account for achieving the ultimate polarizations.

1. Frequency Modulation effect (FM).

A strong increase of polarization by a dramatic factor of 1.7 due to frequency modulation (FM) was discovered in D-butanol doped with paramagnetic Cr(V) complex which was the material used in the large 1.5 l target of the SMC-collaboration at CERN [1, 2]. FM is regularly used for the achievement of the highest polarizations. Dynamic nuclear polarization (DNP) is obtained by microwave (MW) saturation of the electron paramagnetic resonance (EPR) line of the dopant diluted in the target material. The efficiency of the method depends on intensity and spatial uniformity of MW field in a target cavity. At 2.5 T field the typical MW wavelength of $\lambda \approx 4$ mm is smaller than the target dimensions and the cavity field exhibits a standing wave structure. Polarization will be higher in the domains having larger paramagnetic absorptions in comparison to those in which there are the maxima of dielectric losses (so-called hot spots). To equalize a spatial saturation, the field maxima should be spread out over the material volume for a short enough time interval.

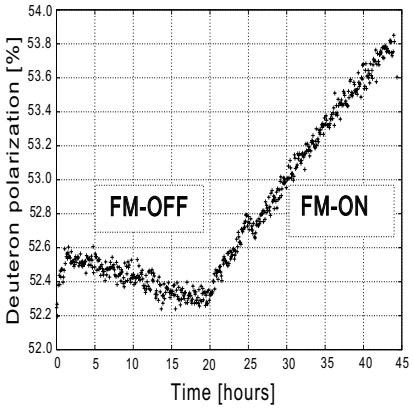

Figure 1. DNP-process in LiD over time with and without FM.

The novelty of FM-invention consists in the mechanism of MW field displacement by sweeping over the modes, in other words, by multi-mode excitation of the cavity [3]. For

this, the carrier MW frequency is slightly modulated with an external modulation of about 20 MHz width. It was shown [3] that if the cavity design enables 3 to 4 non degenerate modes per 20 MHz frequency band, then FM provides a good spatial uniformity of the field as required for the highest polarizations. Following this way one can enlarge the fraction of the nonlinear (with respect to the input power) resonant magnetic losses in comparison with linear dielectric losses. Fig. 1 shows FM-action in case of the COMPASS LiD-target. Polarization went down when switching-off FM and it was growing up to ultimate values when restarting FM.

2. Line shape asymmetry.

The NMR line shape of polarized nuclei usually reveals an asymmetry which contains useful information about the status of the spin system. Fig. 2a shows the spectra of highly polarized deuterons ($S = 1$) in D-propanediol and D-butanol obtained at Bochum University [4]. Deuteron asymmetry of these spectra arises due to an interaction between the nuclear quadrupole moments and the electrical field gradient in the lattice. This interaction contributes to a quadratic term in the sublevel energies.

In an amorphous solid material, the energy of $S = 1$ spin system in a magnetic field can be introduced as [5]

$$E_m = E_0 - E_1 m + E_2(\theta) m^2 \,, \tag{1}$$

where m is magnetic quantum number, E_0 - doesn't depends on the spin, $E_1 = h\nu_D$ is the Zeeman energy and $E_2(\theta) = 3h\nu_q(3\cos^2\theta - 1)$ is the quadrupole energy, dependent on the angular distribution of the molecules about the magnetic field. In practice, the signal asymmetry R is handy to express in terms of relative populations p_m $(m = +1, 0, -1)$

$$R = \frac{p_+}{p_0} = \frac{p_0}{p_-} = \frac{p_+ - p_0}{p_0 - p_-} \,. \tag{2}$$

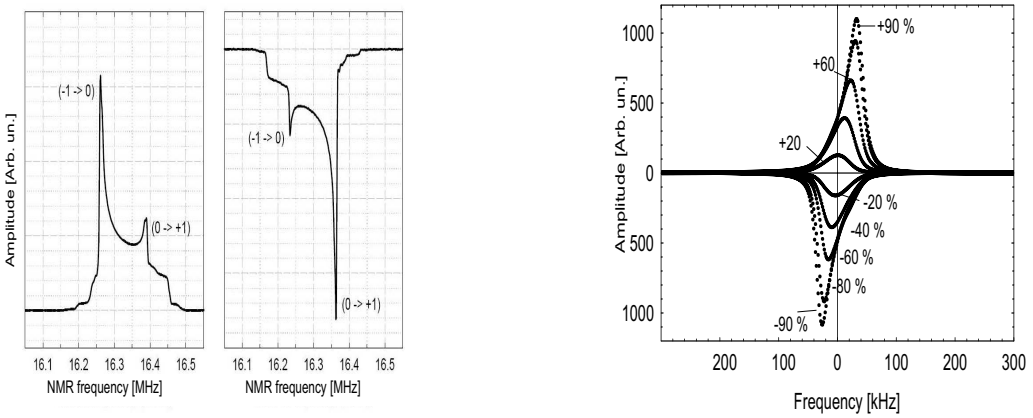

Figure 2a. NMR-signals of D-propanediol (left) and D-butanol (right) with record polarizations of -81 % and +80 %, respectively [4]
Figure 2b. Proton spectra in NH_3 with different polarizations from -90 % to +90 % [8].

Using Eqs. 1, 2 and Boltzmann distribution for sublevels, we have [5]

$$R(\theta) = \frac{\exp(x-y)-1}{1-\exp-(x+y)}\ ,\quad x = \frac{E_1}{kT}\ ,\quad y = \frac{E_2(\theta)}{kT}\ . \tag{3}$$

where kT is the Boltzmann factor, E_2 gives nonequidistant splitting of sublevels. Let us estimate the quadrupole effects for spectra in Fig. 2a. Their maxima are situated at $\theta = \pi/2$, then Eqs. 1 yields $E_2(\theta = \pi/2)/E_1 = -3\nu_q/\nu_D$ and a signal asymmetry at low polarization ($T \to \infty$) equals to

$$\lim_{T\to\infty} R(\theta) = \frac{1 - E_2(\theta=\pi/2)/E_1}{1 + E_2(\theta=\pi/2)/E_1} = \frac{1+3\nu_q/\nu_D}{1-3\nu_q/\nu_D}\ . \tag{4}$$

The value of $3\nu_q/\nu_D$ is the relative shift of the deuteron peaks about the central Larmor frequency; from Figs. 2a this shift is equal to about 55 kHz/16300 $kHz \cong 3.4 \cdot 10^{-3}$ and Eq. 4 gives unity with accuracy of 0.7 %, therefore $E_2 \cong 0$ in Eq. 1 is a good approximation and a signal asymmetry vanishes at low polarizations. The asymmetry can be calculated by formula [6]

$$R(\theta) = \frac{S_{+1} - S_0/\sqrt{2}}{S_{-1} - S_0/\sqrt{2}}\ , \tag{5}$$

where S_{+1} is the right and S_{-1} is the left peak amplitude of the signals in Figs. 2a; S_0 is the amplitude of the medial point between these peaks. From Fig. 2a (left), they are $S_{+1}/S_0 \approx 1.3$, $S_{-1}/S_0 \approx 3.5$ and from Eq. 5 $R \approx 0.59/2.8 = 0.21$; also repeating the same calculations for the spectrum of Fig. 2a (right), we find $R \approx 5.5$. Since $E_2 \approx 0$, from Eqs. 2 it follows the well known formula for the polarization of $S = 1$ spin system [7]

$$P = p_+ - p_- = \frac{R^2-1}{R^2+R+1}\ , \tag{6}$$

which gives of -77 % and +78 % polarizations, as compared with more precise "area method" measurements of -81 % and +80 % in Figs. 2a (left) and 2b (right), respectively.

In contrast with the previous consideration, ^{14}N spins (S=1) in the ammonia exhibit a broadened NMR-spectra ($3\nu_q/\nu$=1.23 MHz/6.47 MHz=0.19) at 2.1 T, $S_0 \approx 0$ [8] and $R = 1.46$ for the limit in Eq. 4. In this case the quadrupole interaction will bring along a strong line shape asymmetry even at the lowest nitrogen polarizations .

Fig. 2b shows another example of asymmetry of the proton spectra in ammonia (NH_3) parametrized over polarization [8]. One can see again a strong line shape asymmetry increasing with polarization. Our preliminary analysis allows to conclude that the asymmetrical part of these spectra vary linearly with polarization. If further studies confirm this finding then the proton polarization in ammonia could also be determined by the signal asymmetry along with the routine "area method".

3. Spin-Spin Cross-Relaxation.

DNP in ammonia at 2.5 T and about 0.1 K allows to reach polarizations of about 14 % and 90 % of ^{14}N and ^1H spins, respectively. As stated above, the nitrogen spins ($S = 1$) have a strong quadrupole interaction with the lattice field. Unlike ^{14}N nuclei, the energy of the half-integral ^1H spins depends only on the magnetic field, so that, by ramping

down the field from 2.5 T to about 0.056 T [8], one can equalize resonant frequencies of both species. At such a field, flip-flop interactions conserve the total energy, allowing an effective cross-relaxation between subsystems. We estimate cross-relaxation time as $\tau = W^{-1}$, where W is an approximate rate of cross-polarization [9]

$$\tau = W^{-1} \approx T_2(\frac{\gamma_H}{\gamma_N})^2 \cosh(\xi\frac{\Delta_0}{\Delta_H}) \ . \tag{7}$$

Here $T_2 \approx 10^{-5}$ s is the transverse relaxation time of proton spins, $\Delta_H \approx 0.05$ MHz is the proton NMR line width, $\gamma_H/\gamma_N = 13.8$ is the ratio of gyromagnetic constants, $\xi \approx 1$ is a free parameter and Δ_0 is the frequency detuning between ^{14}N and ^1H spins. One can see from Eq. 7 that for small detuning of $\Delta_0 \approx \Delta_H$ τ is of the order of $T_2(\gamma_H/\gamma_N)^2 \approx 2\cdot 10^{-3}$ s. In the case of broaden ^{14}N-spectral line, the detuning range is also broadened out within interval of $\Delta_H \approx 0.05$ MHz $< \Delta_0 < 3\nu_q \approx 1.23$ MHz. As a consequence, τ in Eq. 7 can vary from milliseconds to hundreds of seconds depending on the field setting. Studies done at CERN [8] confirm this conclusion. Different cross-relaxation tests allowed to gain the vector polarization of ^{14}N up to 40 % or they destroyed the equilibrium spin distribution. Cross-relaxation can be suppressed by replacing ^{14}N by the ^{15}N isotope. This isotope has spin $S = 1/2$ and $\gamma_H/\gamma_{15N} \approx 9.9$ with no quadrupole effects. In this case the cross coupling effects will vanish at a field larger than 0.05 T.

4. Self-induced spin spectroscopy.

NMR and EPR spectra are usually studying a response of a spin system to an external field excitation within their Larmor frequency [10]. Here, we consider the self-induced spectroscopy of negatively polarized, better saying, active spins without exciting field.

Fig. 3a shows an equivalent resonant circuit coupled with active spin media situated inside the coil which axis is perpendicularly directed about the field (B_0). In this circuit the coil resistance (r) is counterbalanced by the sample energy so that $r = -\eta\omega\chi'' L_0$ and the coil reactive impedance equals to

$$Z = r + j\omega L_0(1 + \eta(\chi' - j\chi'')) = j\omega L_0(1 + \eta\chi'(\omega)) \ , \tag{8}$$

where $j = \sqrt{-1}$, η, r, L_0, $\omega = 2\pi\nu$, $\chi' - j\chi''$ are the coil filling factor, resistance, inductance, the circuit resonant frequency and a sample susceptibility, respectively.

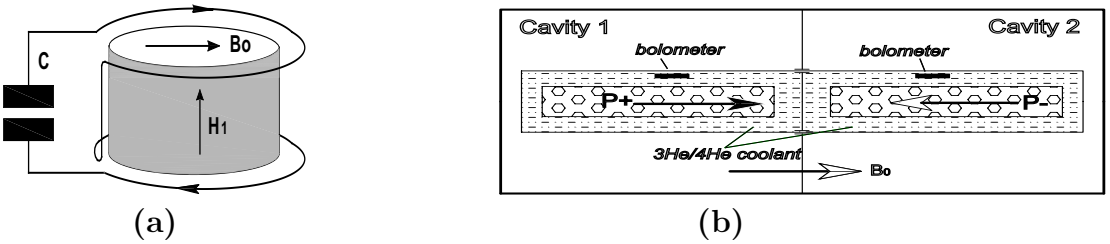

(a) **(b)**

Figure 3a. A circuit coupled with the active media looses a resistance and it acts as a transformer of any external flux deviations into ringing resonant current, generating H_1-field.
Figure 3b. Twin-cavity with opposite target polarizations. The electromagnetic radiation is detected by the temperature disbalance between bolometers (Speer-220).

For example, in the case of a sample made of frozen ammonia bits with a density of $N \approx 5.4 \cdot 10^{28}$ spin/m^3, the averaged value of $\overline{\chi''} = -\pi\chi_0\nu/2\Delta_H$, where χ_0 is the static magnetization. Eq. 8 holds when coil impedance is less than

$$r = -\eta\{\overline{\chi''}\}\omega L_0 = 0.5 \cdot \{\frac{\pi}{2}\frac{\nu_H}{\Delta_H}\frac{N\mu_0\mu_B}{B_0}\}\omega L_0 = 13\ Ohm\ . \tag{9}$$

Here $\mu_0 = 4\pi \cdot 10^{-7}$ H/m is the permeability of vacuum, $\mu_B = 5.0 \cdot 10^{-27}$ J/T is the nuclear magneton and we assume $\eta \approx 0.5$, $\nu \approx 10^8$ Hz at $B_0 = 2.5$ T, $\Delta_H = 5 \cdot 10^4$ Hz, $L_0 = 10^{-7}$ H and proton polarization of 100 %. Since typical coil resistance of $(1 \div 3)$ Ohm $\ll r$ the lossless (superconducting) circuit will transform any flux deviations through the coil into a ringing current generating H_1-field (see Fig. 3a). In turn, the H_1-flux feedback will change the sample susceptibility and the coil inductance (see Eq. 8), self-tuning of the circuit and the Larmor spin frequencies to a resonance; in full analogy with "pulling effect" in laser technique [12].

One can see that it should exist a particular "self-induced spectroscopy" which operates without an external excitation, with self-tuning to a circuit resonance, with direct indication of electromagnetic radiation using the extra low-noise cryo-bolometers; it is true, on the other hand, that the method can not be realized without an active media.

Our set-up [13] shown in Fig. 3b consists of the two electrically isolated MW cavities with oppositely polarized LiD-material in cells. The two resonance circuits enable radiation: NMR-circuits for polarization measurements and the MW cavity. The studies were performed with LiD at low fields of ≈ 0.1 T, where NMR circuits have not any resonance for Larmor frequencies for all nuclear species, therefore only electron spins can activate the radiation in the microwave cavity. This radiation will unbalance the bolometer temperatures which were measured by the low-frequency cryo-bridges.

The fast electromagnetic energy release, shown in Fig. 4a [11], with $\tau_f \approx 18$ min originated by electron spins coupled through the electron dipole-dipole reservoir [7] with Zeeman reservoir of negatively polarized nuclear species in LiD. It is most probable that the generation goes in TM_{002} or TM_{022} modes of our cavity having a large radius of

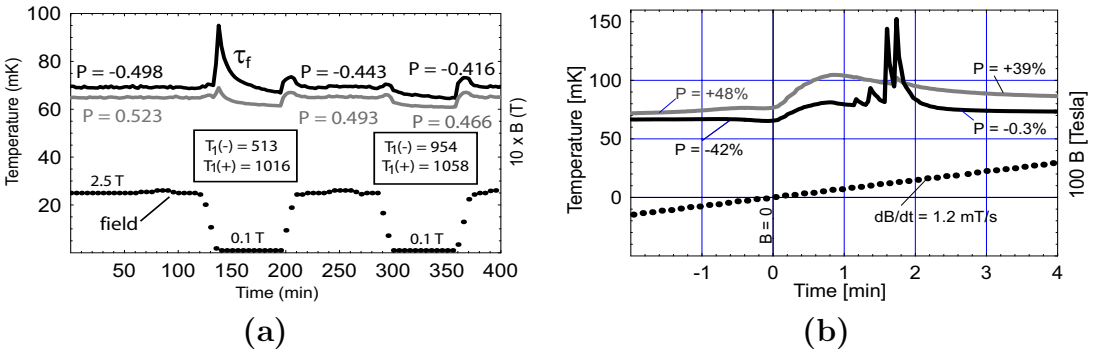

Figure 4a. Bolometer detects a fast release of spin energy with $\tau \approx 18$ min. After the exposure, NMR-reading confirms the different relaxation times $T_1(-) \ll T_1(+)$ (in hours) for opposite polarizations. This effect vanishes at the lower polarization in the second exposure [11].
Figure 4b. Specified spectrum from [11]; the specra-resolved spin-radiation (from the left to right): ^1H (90), ^7Li (101), D (121) and ^6Li (127) mT.

10.5 cm with the low resonant frequencies in region of 2.5÷ 3.5 GHz and a large quality factor of the order of 10^4. Such radiation means that nuclear spins can relax their energy over a broad-band microwave noise due to their dipole-dipole contact with electron spins.

Figure 4b shows the first observation of the spectra-resolved radiation during reversal of B_0-magnetic field [11]. In this case, radiation discloses the individual contributions of nuclear species into the electron dipole-dipole reservoir.

In conclusion, we hope that our observations may provide useful information to a deeper understanding of self-induced processes in polarized spin systems.

Acknowledgment.

Authors would like to thank all members of SMC and COMPASS collaborations at CERN who participated in the new studies of spin phenomena in polarized target materials.

References

[1] Yu. Kisselev (On behalf of SMC Collaboration), NIM in Phys. Res., A 356, 99, 1995;

[2] B. Adeva, A. Magnon et al., NIM in Phys. Res., A 372, 339, 1996;

[3] Yu. Kisselev et al., Proc. of the 11th International Workshop on Polarized Sources and Targets, Tokyo, Japan,14-17 Nov., 63, (2005);

[4] S. T. Goertz et al., NIM in Phys. Res., A 526, 43, 2004;

[5] L. I. Lapidus, JINR Preprint, Dubna, **P2-84-267**, 1984.

[6] Yu. Kisselev, S. A. Popov, A. N. Fedorov, Pys'ma Zh. Eksp. Teor. Fiz., **55**, 99 (1992).

[7] W. de Boer, Dynamic Orientation of Nuclei at Low Temperatures, Yellow Report, Geneva. **CERN 74-11**,(1974).

[8] B. Adeva and Ch. Dulya et al., NIM in Phys. Res., A 419, 60, 1998;

[9] F. S. Dzeparov, Zh. Eksp. Theor. Fiz., **99**, 982 (1991); Phys. Part. Nucl., **26**, 692 (1995).

[10] A. Abragam, Principles of Nuclear Magnetism (Clarendon Press. Oxford), **Ch. IV, IX**, (1989).

[11] Yu. Kisselev et al., SPIN-2004: proc. of the 16th Int. Spin Phys. Symp. and Workshop on Polar. Electron Sources and Polarimeters, Trieste, Italy, 10-16 Oct., 816, (2004).

[12] R. H. Pantell, H. E. Puthoff, Fundamentals of Quantum Electronics (Wiley, New York, etc), **Ch.3**, 90, (1969).

[13] J. Ball et al., NIM in Phys. Res., A 498, 101, 2003.